

# The role of interface between electron transport layer and perovskite in halogen migration and stabilizing perovskite solar cells with Cs<sub>4</sub>SnO<sub>4</sub>

Bingxin Zhao<sup>1</sup>, Guangda Niu<sup>2\*</sup>, Qingshun Dong<sup>1</sup>, Jing Liu<sup>1</sup>, Nan Li<sup>1</sup>, Jiangwei Li<sup>1</sup>, Liduo Wang<sup>1\*</sup>

<sup>1</sup>Department of Chemistry, Tsinghua University, Beijing, P. R. China

<sup>2</sup>Wuhan National Laboratory for Optoelectronics, Huazhong University of Science and Technology, Wuhan, P. R. China

[guangda\\_niu@hust.edu.cn](mailto:guangda_niu@hust.edu.cn), [chldwang@mail.tsinghua.edu.cn](mailto:chldwang@mail.tsinghua.edu.cn)

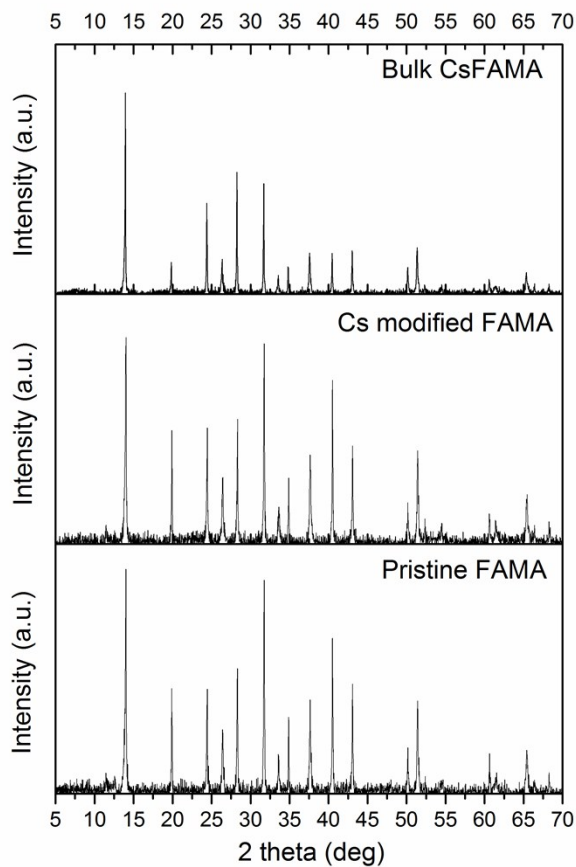


Figure S1. XRD of Pristine FAMA, Cs modified FAMA and bulk CsFAMA.

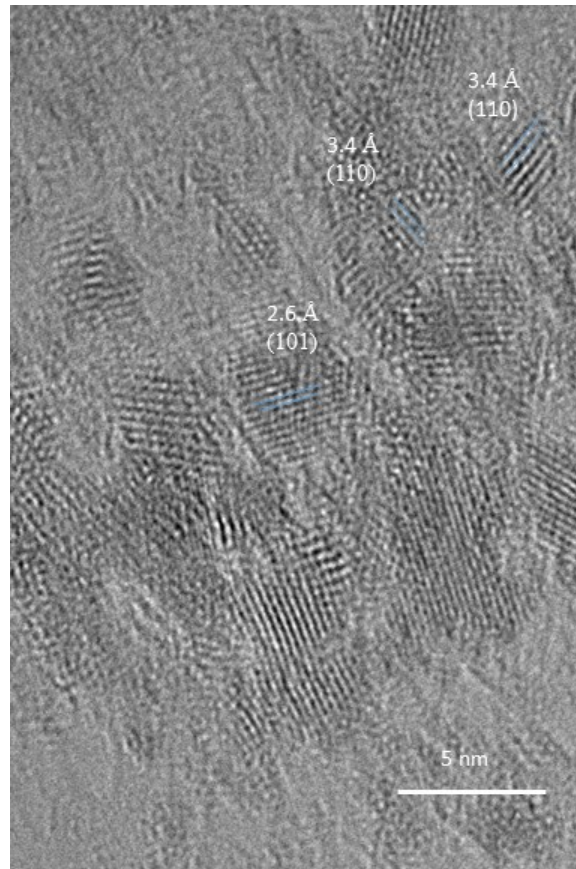


Figure S2. TEM image of SnO<sub>2</sub> nanoparticles.

In order to examine the effect of the interfacial Cs<sub>4</sub>SnO<sub>4</sub> and Cs<sup>+</sup> on the morphology of perovskite, SEM images of pristine FAMA, Cs<sub>4</sub>SnO<sub>4</sub> modified FAMA and bulk CsFAMA are shown in Figure S2. Pristine FAMA and Cs<sub>4</sub>SnO<sub>4</sub>-modified FAMA exhibit larger grain sizes compared with bulk CsFAMA, while the large grain size is beneficial for the crystallinity and device performance.

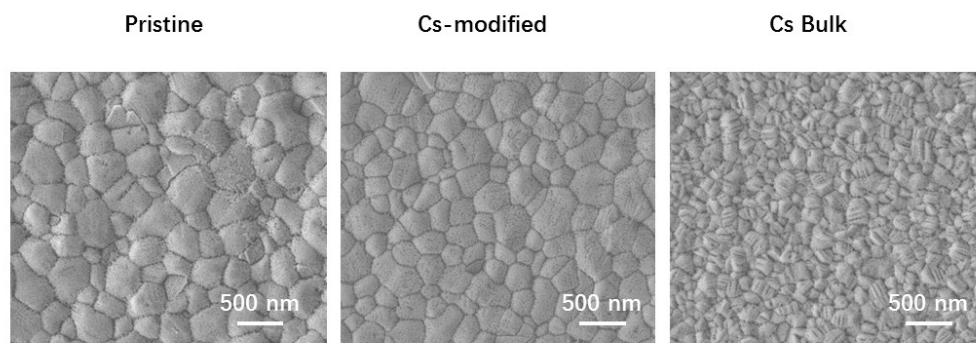


Figure S3. SEM images of pristine FAMA, Cs modified FAMA and bulk CsFAMA.

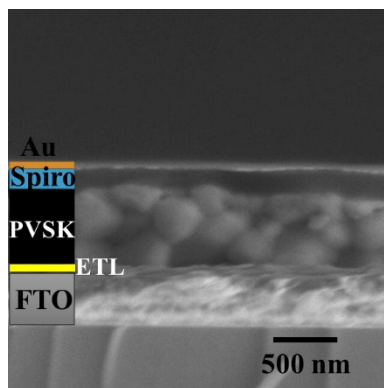


Figure S4. SEM image of a cross section of a complete Cs-modified device.

The depth profiles of  $\text{Br}^+$  for pristine CsFAMA and  $\text{Cs}_4\text{SnO}_4$ -modified device before and after 15 h photoaging are shown in Figure S5. Loss of  $\text{Br}^-$  occurred at the interface of perovskite/ETL. Compare to the loss of  $\text{Br}^-$ , the decrease of I in the control device is more severe (Figure 7), this means I ions are the species most likely to release from perovskite.

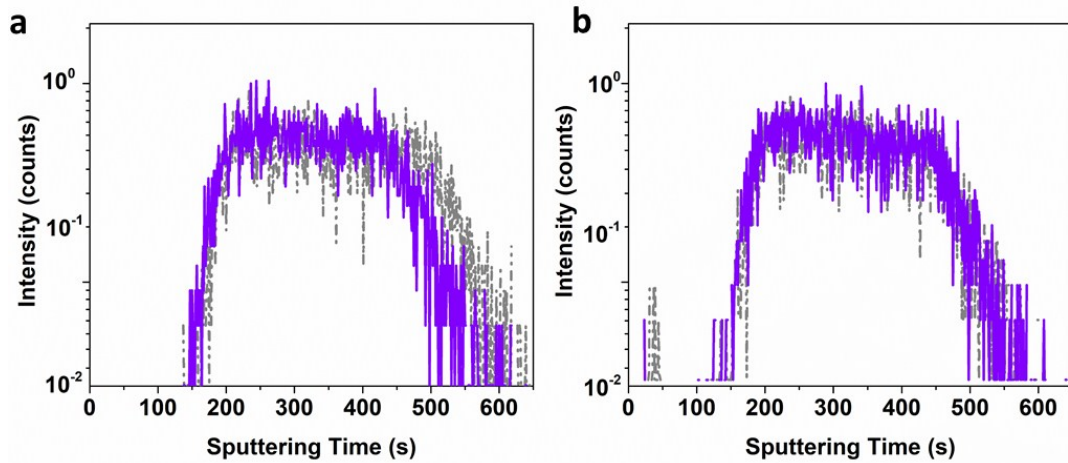


Figure S5. Normalized ToF- SIMS elemental depth profiles of  $\text{Br}^+$  for a) Pristine CsFAMA and b)  $\text{Cs}_4\text{SnO}_4$ -modified device. Grey line: before photoaging; purple line: after 15h photoaging.

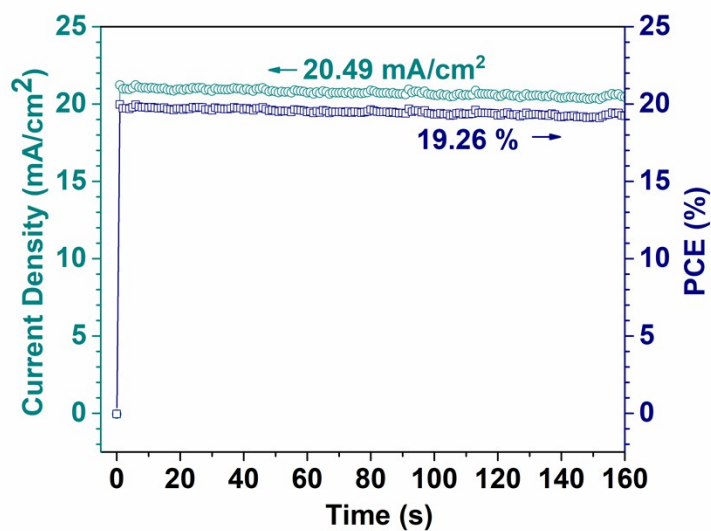


Figure S6. Stabilized current density and PCE of Cs-modified device.

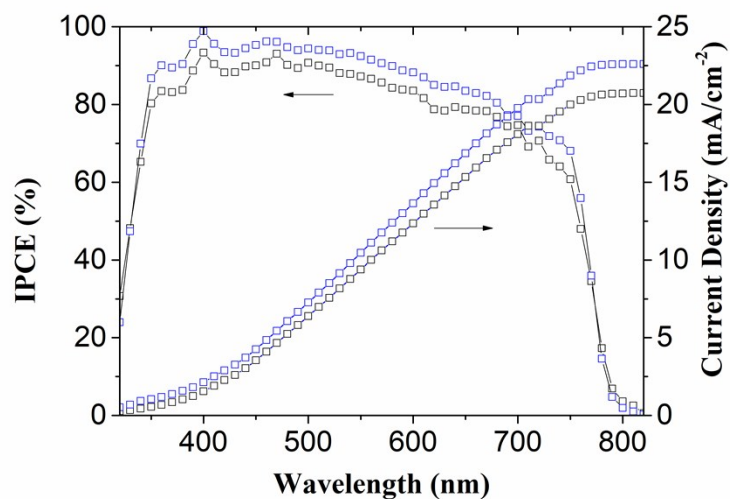


Figure S7. IPCE spectra and integrated current density of the pristine and Cs-modified device.

Table S1. The photovoltaic parameters and hysteresis effect index ( $H_i$ ) of the CsFAMA devices.

Device	Scan direction	$J_{SC}$ (mA/cm <sup>2</sup> )	$V_{OC}$ (V)	FF (%)	Eff. (%)	$H_i$
CsFAMA	R	21.30	1.15	0.70	17.07	0.083
	F	21.26	1.16	0.65	16.02	

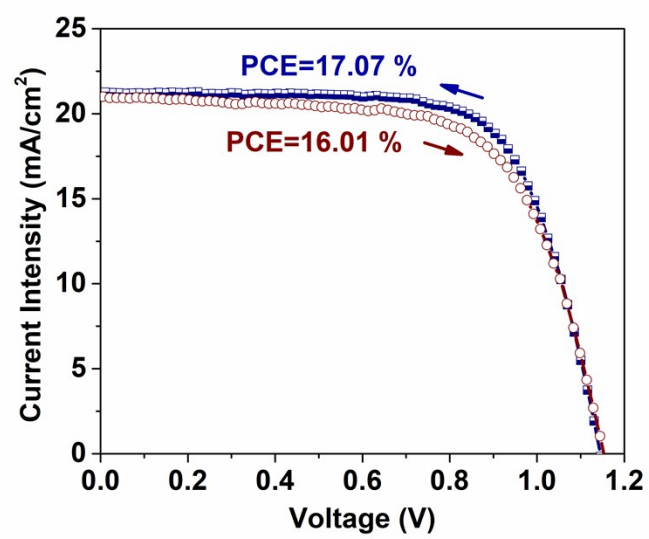


Figure S8. J-V Curves of CsFAMA performed with F/R scan.

Table S2. Complete photovoltaic parameters of pristine device.

		<b>J<sub>SC</sub>(mA/cm<sup>2</sup>)</b>	<b>V<sub>OC</sub>(V)</b>	<b>FF</b>	<b>Eff.(%)</b>
<b>Pristine reverse</b>	1	21.85746	1.12875	0.679206	16.75712
	2	22.22868	1.12875	0.69716	17.49217
	3	22.69813	1.14445	0.69508	18.05599
	4	22.35994	1.12875	0.690885	17.4371
	5	22.52158	1.14445	0.672514	17.33393
<b>Pristine forward</b>	1	21.68932	1.1347	0.65501	16.12041
	2	22.11881	1.15045	0.66637	16.95675
	3	22.65756	1.15045	0.63056	16.43649
	4	22.28319	1.15045	0.63409	16.25538
	5	22.53003	1.15045	0.62316	16.15206

Table S3. Complete photovoltaic parameters of Cs<sub>4</sub>SnO<sub>4</sub>-modified device.

		<b>J<sub>SC</sub>(mA/cm<sup>2</sup>)</b>	<b>V<sub>OC</sub>(V)</b>	<b>FF</b>	<b>Eff.(%)</b>
<b>Cs<sub>4</sub>SnO<sub>4</sub>- modified reverse</b>	1	22.6538	1.14445	0.71347	18.49752
	2	22.8016	1.16015	0.72003	19.04715
	3	22.82245	1.16015	0.706658	18.7105
	4	22.52173	1.16015	0.692653	18.09804
	5	22.81529	1.16015	0.726435	19.22814
<b>Cs<sub>4</sub>SnO<sub>4</sub> - modified forward</b>	1	22.58385	1.15045	0.68654	17.83743
	2	22.79562	1.15045	0.68352	17.92542
	3	22.72954	1.16625	0.69654	18.46404
	4	22.43222	1.16625	0.69031	18.05963
	5	22.76402	1.15045	0.70022	18.33799